# Active Distribution Network (ADN) Grid Structure Optimization and Flexible Resource Collaborative Planning for High-Proportion Renewable Energy Consumption

DOI: 10.23977/fpes.2025.040110 ISSN 2516-2926 Vol. 4 Num. 1

Jin Panlong<sup>1,a</sup>, Yang Zhao<sup>1,b</sup>, Wang Zhiyuan<sup>2,c,\*</sup>

<sup>1</sup>Economic and Technical Research Institute, State Grid Ningxia Electric Power Co., Ltd., Yinchuan, Ningxia, China

<sup>2</sup>Tianjin University, Nankai, Tianjin, China

<sup>a</sup>2698830118@qq.com, <sup>b</sup>2725415389@qq.com, <sup>c</sup>xhl110302@126.com

\*Corresponding author

*Keywords:* ADN; Renewable Energy Absorption; Grid Optimization; Flexible Resources; Collaborative Planning

Abstract: Active distribution networks (ADN) designed to accommodate high-proportion renewable energy consumption face challenges such as insufficient grid structure flexibility, power flow fluctuations, and voltage over-limits at high renewable energy penetration rates. Optimizing the grid structure and coordinating flexible resource planning are urgently needed to improve system absorption capacity and operational safety. This paper constructs a multi-objective planning model based on source-grid-load-storage coordination, incorporating grid structure optimization, distributed energy storage configuration, and adjustable load scheduling into a unified framework. The objective function covers maximizing the renewable energy absorption rate, minimizing operating costs, and voltage deviation constraints. The steps include: (1) establishing a time series model that considers distribution network trends and uncertainties; (2) introducing a typical scenario generation method to characterize renewable energy output fluctuations; (3) constructing a mixed integer linear programming to coordinately optimize grid reconstruction, energy storage layout, and flexible load scheduling; (4) using an improved genetic algorithm for solution and designing a multi-scenario iterative convergence mechanism. Case studies show that compared to a traditional fixed grid structure, the optimized system's renewable energy absorption rate increases to 93%, with average daily operating costs as low as \pmex9800, and the average voltage over-limit probability decreases to 3.01%, significantly enhancing the flexibility and clean energy utilization of ADN.

#### 1. Introduction

The high proportion of renewable energy integration has profoundly changed the operational characteristics of ADNs. Distributed photovoltaic and wind power output exhibits significant volatility and intermittency. Combined with load-side uncertainties, the system faces challenges

such as voltage excursions, repeated power flow fluctuations, and localized grid constraints. Relying solely on traditional architectures often makes it difficult to maintain stable operations. ADNs urgently need to develop new coordination mechanisms that leverage grid structure flexibility and resource adjustability to ensure the full absorption and efficient transmission of clean energy within the network.

In this context, it is crucial to comprehensively consider the multi-dimensional factors of power generation, grid, load, and storage for joint scheduling and planning. The reconfigurability of the grid structure provides spatial flexibility, the transferability of energy storage can balance time-series differences, and adjustable loads enable optimized coordination on the load side. By establishing a multi-objective optimization model that integrates absorption capacity, economic efficiency, and voltage safety into a unified framework, it can provide system-level support for ADN in an environment with an increasing proportion of renewable energy.

This paper constructs a mixed-integer linear model that incorporates grid optimization, energy storage placement, and load regulation, and introduces an improved genetic algorithm and a multi-scenario generation strategy to solve the problem, achieving a dual integration of modeling and algorithmic approaches. This unified framework balances the absorption of renewable energy and operational safety, demonstrating a technical approach for optimizing ADN operations under conditions with a high proportion of renewable energy. A case study verifies the effectiveness and engineering value of the research approach.

#### 2. Related Work

Research on ADN has been carried out in different directions, involving grid structure optimization, distributed resource allocation and digital modeling methods. Different research entry points emphasize multi-level exploration from power electronic devices to probabilistic modeling and multi-attribute evaluation, forming a relatively rich reference system. Liu et al. proposed a multi-objective collaborative optimization method for DC distribution network grid structure and DPV [1]. This method considers the correlation between photovoltaic output and load power uncertainty factors, uses a two-dimensional Gaussian mixture model to model the source-load joint probability distribution, and constructs a typical scenario set by the acceptance-rejection sampling method. In order to absorb distributed energy such as photovoltaics, electric vehicles, and energy storage batteries and realize the optimal distribution of power in the distribution network, Xiao et al. proposed an AC/DC intelligent distribution network structure based on power electronic flexible devices [2]. Chen et al. took the distribution network planning of multiple regions as the research object, and used the proposed hybrid multi-attribute evaluation optimization model to analyze the optimal grid suitable for construction under the differentiated needs of different regions, and verified the effectiveness of the proposed model [3]. Zhang et al., based on the inspiration of the advanced power grid in Paris, France, proposed relatively clear definitions of "strong, simple, and weak" for high and medium voltage distribution networks, and established a set of typical coordination scheme optimization models for high and medium voltage distribution network structure based on safety, reliability and economic evaluation [4]. Wen et al. defined the concept of load release and proposed a distribution network grid structure economic calculation model that takes into account the load release process [5]. The model takes into account the dynamic operating network loss and power outage loss of the distribution network during the load release process, and quantitatively evaluates the economic efficiency of the distribution network grid structure from the perspective of the overall planning period. Xu et al. proposed a grid mapping edge computing structure to drive the emerging digital distributed distribution network [6]. Deka et al. summarized and compared recent research results on distribution network topology identification and detection schemes, and established effective connections between them [7]. Stefenon et al. proposed using segmentation and edge detection techniques to expand the database, so that classification can be performed using the Inception v3 deep neural network model [8]. Jiang et al. identified and compared the topological structure of SOP as a multifunctional power electronic device, including back-to-back voltage source converter, multi-terminal voltage source converter, unified power flow controller and direct AC-AC modular multilevel converter [9]. Helmi et al. proposed a novel and effective optimization framework to solve the reconstruction problem of modern distribution networks [10]. Although existing studies have proposed a variety of methods, they often lack systematicity in source-grid-load-storage coupling modeling and global optimization mechanisms. This paper constructs a unified multi-objective framework and combines it with an improved genetic algorithm to seek an overall balance between absorption, economy and voltage stability.

# 3. Methodology

# 3.1 Objective Function Setting

The goal of maximizing the renewable energy consumption rate is achieved by calculating the ratio of actual grid-connected renewable energy power to the total renewable energy power that can be generated, defined as:

$$F_1 = \max \frac{\sum_{t \in T} P_t^{RES,used} \cdot \Delta t}{\sum_{t \in T} P_t^{RES,avail} \cdot \Delta t} (1)$$

 $P_t^{RES,used}$  is the renewable energy output utilized in period t, and  $\sum_{t \in T} P_t^{RES,avail}$  is the renewable energy output available in that period. The goal of operating economy is modeled by the total system operating cost, which includes the electricity purchase cost, energy storage operation expenditure and line loss, and is expressed as [11]:

$$F_2 = \min \left( \sum_{t \in T} C_t^{\text{buy}} P_t^{\text{grid}} \Delta t + \sum_{i \in S} C_i^{\text{stor}} \left( P_{i,t}^{\text{ch}} + P_{i,t}^{\text{dis}} \right) \Delta t + \sum_{l \in L} C_l^{\text{loss}} P_{l,t}^{\text{loss}} \Delta t \right) (2)$$

 $C_t^{buy}$  is the electricity purchase price in the electricity market,  $P_t^{grid}$  is the exchange power with the upper grid, and  $C_i^{stor}$  is the energy storage unit operating cost coefficient.  $P_{i,t}^{ch}$ ,  $P_{i,t}^{dis}$  represent the energy storage charging and discharging power, respectively, and  $C_l^{loss}$  incorporates the line loss price. The voltage quality constraint uses the deviation of each node voltage from the rated value as a penalty term, expressed as:

$$F_3 = \min \sum_{t \in T} \sum_{n \in N} w_n |V_{n,t} - V^{ref}| (3)$$

 $V_{n,t}$  is the voltage amplitude at node n during time period t,  $V^{ref}$  is the rated voltage, and  $w_n$  is the penalty weight. These three objectives are jointly solved through a weighted or hierarchical optimization approach to achieve a multi-objective optimization result: maximizing renewable energy output, minimizing operating costs, and stabilizing voltage levels.

# 3.2 Specific Steps

### 3.2.1 Constructing a Time Series Model Including Power Flow and Uncertainty

The time series model needs to describe the power balance and network status of the distribution network in each discrete time period, and take into account the random fluctuations of renewable energy and load. The power flow calculation of the distribution network is based on branch currents, and the relationship between node injection power and voltage amplitude is expressed as:

$$P_{n,t} + jQ_{n,t} = V_{n,t} \sum_{m \in \Omega_n} \left( \frac{V_{n,t} - V_{m,t}}{Z_{nm}} \right)^* (4)$$

 $P_{n,t}$  and  $Q_{n,t}$  are the active and reactive power injections into node n during period t,  $V_{n,t}$  is the node voltage,  $Z_{nm}$  is the line impedance, and  $\Omega_n$  represents the set of nodes adjacent to node n[12]. Uncertainty is introduced through scenario-based methods. New energy power and load levels are generated by sampling using probability distributions to ensure that different scenarios can cover typical daily operating patterns. The constraint relationship is:

$$P_{t,s}^{RES} \!\!=\!\! \boldsymbol{\widehat{P}}_{t}^{RES} \!\!+\!\! \boldsymbol{\varepsilon}_{t,s}, \! \boldsymbol{P}_{t,s}^{Load} \!\!=\!\! \boldsymbol{\widehat{P}}_{t}^{Load} \!\!+\!\! \boldsymbol{\delta}_{t,s}(5)$$

 $P_{t,s}^{RES}$  represents the output of scenario s at time period t,  $\hat{P}_t^{RES}$  and  $\hat{P}_t^{Load}$  are predicted values, and  $\epsilon_{t,s}$  and  $\delta_{t,s}$  represent the random disturbances under scenario s. By combining power flow balance constraints with scenario-based load and output data, the system's operating state can be fully characterized for each time period and scenario.

# 3.2.2 Characterizing Renewable Energy Volatility Using Representative Scenario Generation

Renewable energy volatility modeling relies on historical output data and forecast results, converting high-dimensional random sequences into a limited number of representative scenarios to reduce computational complexity. A large number of candidate sequences are obtained through Monte Carlo sampling, and then grouped using K-means clustering. Each group of samples is represented by a typical day, expressing the characteristics of renewable energy output under different operating conditions [13]. The similarity between the candidate scenario and the typical scenario is measured using the Euclidean distance, which is defined as:

$$d_{s,k} = \sqrt{\sum_{t \in T} (P_{t,s}^{RES} - P_{t,k}^{RES})^2}$$
 (6)

 $P_{t,k}^{RES}$  represents the representative output corresponding to the cluster center. After clustering is completed, the probability of occurrence of each typical scenario is obtained based on the sample ratio, expressed as:

$$\pi_k = \frac{|S_k|}{\sum_i |S_i|} (7)$$

Period	Scenario 1	Scenario 2	Scenario 3	Scenario 4	Scenario 5
1	0.05	0.10	0.08	0.12	0.07
2	0.20	0.25	0.22	0.28	0.18
3	0.55	0.60	0.62	0.58	0.50
4	0.88	0.92	0.95	0.85	0.90
5	0.70	0.75	0.72	0.78	0.68
6	0.15	0.18	0.20	0.22	0.16

Table 1: Typical PV Output Data

 $|S_k|$  is the number of samples in the cluster. This approach not only reduces the number of scenarios but also preserves the statistical characteristics of renewable energy fluctuations. Table 1 presents typical PV output data, including normalized results for six time periods and five typical scenarios, reflecting the differences between morning and evening troughs and midday peaks.

This table shows the distribution of output differences across different scenarios, which can be used for probability-weighted calculations in subsequent optimization.

# 3.2.3 Establishing a Mixed Integer Linear Programming Model to Handle Multivariate Optimization

The mixed integer linear programming model introduces Boolean variables on top of continuous variables to characterize the switchability of the grid structure and the start/stop states of flexible resources. This allows for a unified description of power flow constraints, equipment operating boundaries, and optimization objectives. The line switch status is represented by a binary variable, which enables the distribution network topology to be dynamically adjusted under different operation schemes and ensures the linear approximation of the network physical laws [14]. The node power balance must be satisfied in each time period and scenario, which is expressed as:

$$P_{n,t,s}^{Gen} + P_{n,t,s}^{Grid} + \sum\nolimits_{i \in \Omega_n} \ P_{i,t,s}^{stor} = P_{n,t,s}^{Load} + \sum\nolimits_{l \in \Omega_n} \ P_{l,t,s}^{flow}(8)$$

 $P_{n,t,s}^{Gen}$  is the node's local renewable energy output,  $P_{n,t,s}^{Grid}$  is the upper grid exchange power,  $P_{i,t,s}^{stor}$  is the energy storage unit charge and discharge power, and  $\Omega_n$  represents the branch or device collection connected to the node. Line loss and current limit are linearized, and line flow switch variables are introduced to ensure reasonable routing. The constraint form is:

$$-P_l^{\text{max}} \cdot y_1 \leq P_{l,t,s}^{\text{flow}} \leq P_l^{\text{max}} \cdot y_1(9)$$

 $y_1$  is a binary variable indicating whether the line is operational, and  $P_1^{max}$  is the rated capacity of the line. In this way, grid structure reconstruction and energy storage and load regulation decisions are integrated into the MILP solution framework, enabling direct constraint solving of the multi-objective optimization function, ensuring both mathematical feasibility and optimality of the results.

# 3.2.4 Introduction of an Improved Genetic Algorithm

When solving mixed-integer linear programming, genetic algorithms use chromosomes to represent grid switching states and energy storage operation strategies. The fitness function is composed of a weighted combination of renewable energy consumption rate, operating costs, and voltage deviation. To avoid falling into local optimality, adaptive crossover and mutation operators are introduced. Specifically, the probability is dynamically adjusted based on the iterative algebra. When the population diversity is insufficient, the mutation rate is increased, and when the convergence trend is obvious, the crossover rate is reduced. The mathematical form of fitness calculation is:

$$Fit(x) = \alpha \cdot \frac{\sum_{t} P_{t}^{RES,used}}{\sum_{t} P_{t}^{RES,avail}} - \beta \cdot C_{op}(x) - \gamma \cdot \sum_{n,t} |V_{n,t} - V^{ref}| (10)$$

 $\alpha,\beta,\gamma$  are the weight coefficients, which represents the operating cost of scheme x. The voltage deviation is calculated as the absolute difference. The selection of parent and offspring is completed by roulette combined with tournament strategy to enhance the replication probability of excellent individuals [15]. The expression of dynamic crossover probability is:

$$p_c = p_{c,min} + (p_{c,max} - p_{c,min}) \cdot \frac{f_{max} - f'}{f_{max} - f_{avg}} (11)$$

f is the fitness of the individuals participating in the crossover,  $f_{max}$  and  $f_{avg}$  are the maximum and average fitness, respectively, and  $p_{c,min}$  and  $p_{c,max}$  are the upper and lower bounds. The final result is a global optimal solution achieved through multiple iterations. The algorithm maintains the search range while improving convergence speed. Table 2 shows the convergence of the mean and

optimal fitness values at different generations of the genetic algorithm.

1					
Generation	Average	Best	Crossover	Mutation	Feasibility
	Fitness	Fitness	Probability	Probability	Rate
10	0.62	0.70	0.82	0.09	91%
20	0.71	0.80	0.78	0.07	94%
30	0.77	0.86	0.74	0.06	96%
40	0.83	0.91	0.70	0.05	97%
50	0.87	0.94	0.66	0.04	98%
60	0.89	0.96	0.64	0.03	99%

Table 2: Convergence of the mean and optimal fitness values

This table shows that individual fitness gradually improves during the iteration process, crossover and mutation probabilities dynamically adjust with changes in diversity, and the solution feasibility rate approaches stability with iteration.

#### 4. Results and Discussion

# 4.1 Example Comparison

# **4.1.1 New Energy Absorption Rate**

The case study selected a 30-node distribution system, using a typical summer daily load curve as the background. The photovoltaic and wind power curves were derived from historical data superposition error simulations. The installed energy storage capacity was set at 20% of the total peak load, and the electricity purchase price was based on a real-time price sequence. This method was compared with a standard genetic algorithm and particle swarm optimization. The runtime covered a 24-hour period, and the available output of renewable energy was generated based on scenario generation. The optimal scheduling solution was solved under different algorithmic frameworks. The effectiveness of each method in improving the absorption rate is shown in Figure 1:

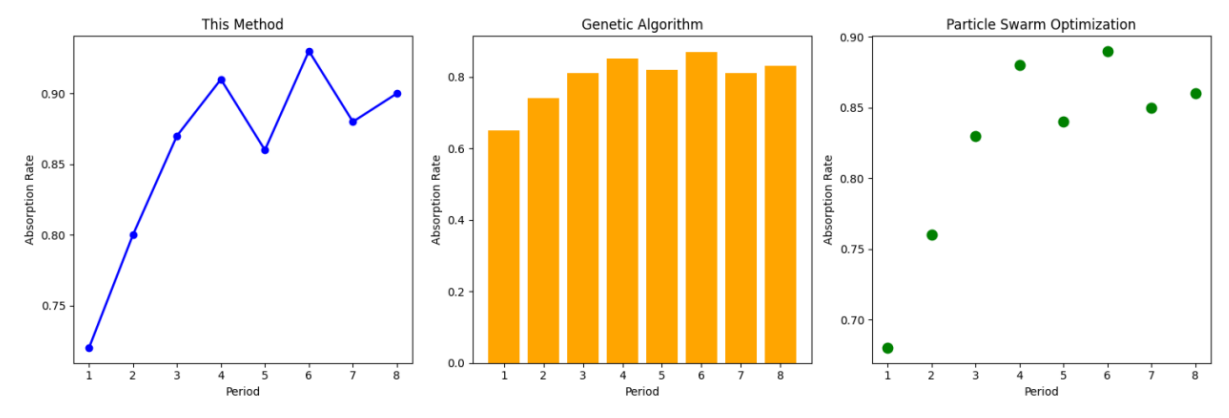


Figure 1: New Energy Absorption Rate

The results show that the differences between the curves of the different algorithms are smaller during low-load periods, but are more pronounced during peak renewable energy output periods. The proposed method achieves an absorption rate of 0.93, significantly outperforming the comparison algorithm, and remains above 0.85 during most periods. This demonstrates that the combination of a mixed-integer linear model and an improved genetic algorithm can effectively achieve resource matching and dynamic topology adjustment, improving the efficiency of

renewable energy utilization during periods of high power output. It also maintains stable performance during periods of fluctuating power output. The comparative method exhibits significant limitations during periods of high power consumption, indicating that its search capabilities are insufficient for globally coordinating energy storage and power purchase selection.

# **4.1.2** System Daily Operating Cost

In the economic performance test, the system still used the same node scale and renewable energy timing curve as input, but the evaluation metric shifted to total operating costs, including electricity purchase expenses, energy storage lifespan loss, and network loss costs. Average daily operating costs were calculated over eight days. To ensure a fair comparison, all algorithm parameters were configured according to commonly recommended values, and the number of iterations and swarm size remained consistent. Therefore, the only differences stemmed from the search mechanism and modeling capabilities. This method was compared with particle swarm and traditional genetic algorithms, and the results are shown in Figure 2.

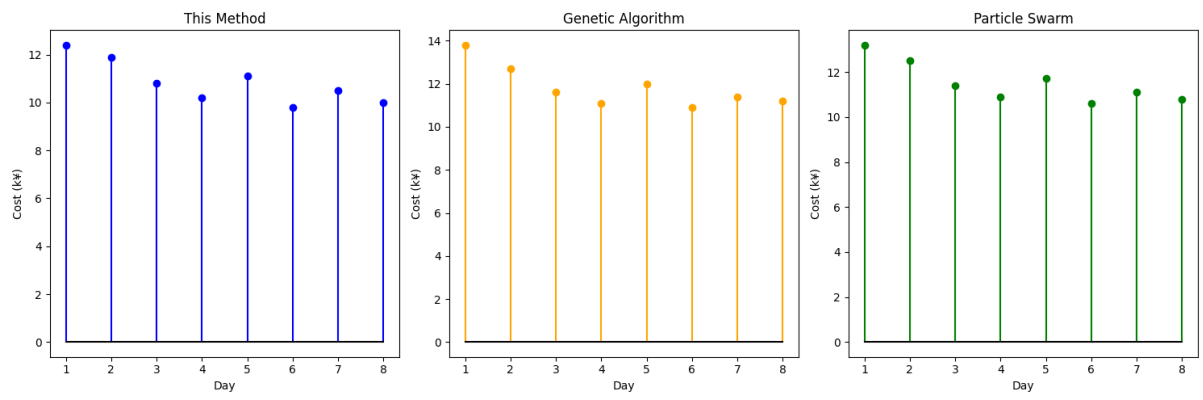


Figure 2: Daily Average Operating Cost (k¥)

This method maintains lower costs than the comparison algorithm during most periods. It also avoids the cost spikes that occur during certain periods due to simply reducing electricity purchases. Instead, it provides a more flexible start-stop combination during peak periods, resulting in a more balanced use of energy storage output. The lowest daily average operating cost reaches \mathbb{Y}9800. The overall operating cost of the genetic algorithm is relatively high, primarily due to the fixed crossover and mutation parameters, which results in slow convergence and prevents some feasible solutions from appearing within a finite number of iterations. The particle swarm algorithm performs slightly better, but lacks a mechanism to break away from local convergence, leading to significant performance differences during the most cost-sensitive morning rush hour. Overall, the improved method's economic advantages complement its improved consumption rate, demonstrating strong overall optimization capabilities.

#### **4.1.3 Voltage Exceeding Probability**

The test was conducted under the same system topology, but with increased load and renewable energy disturbance amplitudes. Multi-scenario Monte Carlo sampling was used to construct randomized cases. Each scenario lasted 15 minutes, and the total sample size was set to 200. Each algorithm independently obtained a scheduling plan and counted whether the node voltage exceeded the rated boundary. The exceeding probability was then calculated to ensure that the results reflect the method's ability to support voltage stability under uncertain shocks. Figure 3 shows the specific results.

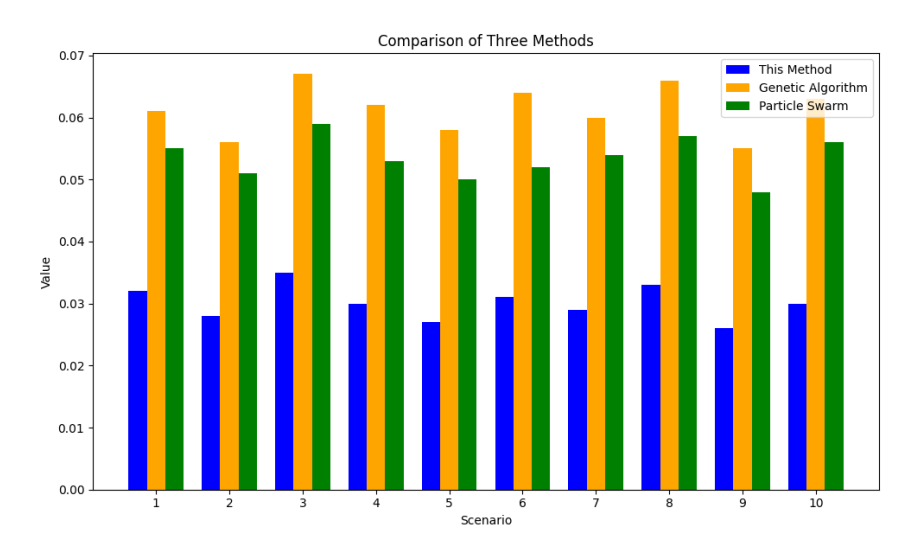


Figure 3: Voltage Exceeding Probability

The average voltage exceeding probability for this method is 0.0301, compared to 0.0612 for the genetic algorithm and 0.0535 for the particle swarm. This indicates that the proposed method reduces the voltage exceeding probability by almost half. This is because the constructed constraint model considers voltage boundaries when adjusting the energy storage and grid topology, reducing local overshoots. The comparative method lacks this global coupling mechanism, making it more likely to exceed the limit in high-disturbance scenarios.

# **4.2 Results Analysis**

A comprehensive example demonstrates the advantages of proposed method across three metrics: renewable energy consumption rate, operational economics, and voltage over-limit probability. First, regarding consumption rate, the improved algorithm not only achieves a maximum utilization rate of 0.93 during peak hours but also maintains a rate above 0.85 during most periods, significantly alleviating wind and solar curtailment. This effectiveness is closely related to the optimization search capability and dynamic topology adjustment. Regarding economic indicators, the average daily cost for eight consecutive days was lower than that of the control method, reaching a minimum of \(\frac{1}{2}\)9800. This demonstrates superior decision-making capabilities based on a multi-objective trade-off, managing both electricity purchase costs and energy storage lifespan. In terms of voltage safety, the average over-limit probability decreased by approximately 51% and 44% compared to the genetic algorithm and particle swarm optimization algorithms, respectively, demonstrating stronger adaptability to uncertainty. This is due to the model's effective incorporation of voltage constraints under random perturbations. Overall, the proposed improved genetic algorithm and MILP coupling framework achieves a balanced approach of increasing the power consumption rate, improving economic efficiency, and balancing voltage safety. Compared to simple search algorithms, it offers substantial improvements in globality and robustness.

#### 5. Conclusion

This paper addresses the operational challenges of ADNs under conditions with a high proportion of renewable energy and proposes a multi-objective optimization framework for source-grid-load-storage collaboration. This framework achieves unified coupling of grid reconfiguration, energy storage configuration, and load scheduling at the model level. At the algorithmic level, it enhances global search and robustness through improved genetic strategies and

scenario iteration mechanisms. Case studies demonstrate that this approach can consistently maintain high absorption levels, superior economic efficiency, and more controllable voltage security in complex operating environments, validating the role of collaborative optimization in improving system flexibility and renewable energy utilization. Compared with traditional methods, the proposed framework not only demonstrates stability across various operational scenarios but also provides a more feasible planning and scheduling approach for ADN operations. However, it should be noted that the model still has limitations in terms of parameter dependence and scenario construction, and uncertainties in actual conditions may be even more complex. Therefore, future research could further incorporate higher-dimensional stochastic modeling and multi-agent collaborative control to expand the method's applicability to ultra-large-scale distribution systems and real-time scheduling.

# **Acknowledgements**

This work was supported by Ningxia Natural Science Foundation 2023AAC03825.

#### References

- [1] Liu Fei, Xiong Xiaoqi, Zha Pengcheng, Huang Heming, Xia Qi, Yu Yingting, Li Xiong. Multi-objective collaborative optimization of DC distribution network structure and distributed photovoltaic [J]. Proceedings of the CSEE, 2020, 40(12): 3754-3764
- [2] Xiao Wenhao, Peng Hui, Liu Xingdong, Zhao Li, Zhang Chengke. Design and research of a distribution network structure based on flexible devices [J]. Power Capacitors and Reactive Compensation, 2022, 43(5): 109-117
- [3] Chen Shijie, Xiang Yue, Liu Junyong, Shen Xiaodong. Hybrid multi-attribute evaluation and optimization model for distribution network structure considering load uncertainty and differentiated demand [J]. Power Automation Equipment, 2020,40(11):24-31
- [4] Zhang Yongbin, Zhang Man, Wang Zhuding, Pang Xianglu, Wei Tingting. Coordinated planning scheme for high and medium voltage distribution network grid structure[J]. Automation of Electric Power Systems, 2021, 45(9): 63-70
- [5] Wen Chengyi, Wang Haisheng, Qiao Huan, Li Sifan, Lu Yi, Zhang Shijian. Economic calculation model of distribution network grid structure considering load release process[J]. Mechanical and Electrical Engineering Technology, 2021,50(5):84-86+90
- [6] Xu Z, Jiang W, Xu J, et al. A Power-Grid-Mapping Edge Computing Structure for Digital Distributed Distribution Networks[J]. IEEE Transactions on Smart Grid, 2023, 15(4): 3432-3445.
- [7] Deka D, Kekatos V, Cavraro G. Learning distribution grid topologies: A tutorial[J]. IEEE Transactions on Smart Grid, 2023, 15(1): 999-1013.
- [8] Stefenon S F, Yow K C, Nied A, et al. Classification of distribution power grid structures using inception v3 deep neural network[J]. Electrical Engineering, 2022, 104(6): 4557-4569.
- [9] Jiang X, Zhou Y, Ming W, et al. An overview of soft open points in electricity distribution networks[J]. IEEE Transactions on Smart Grid, 2022, 13(3): 1899-1910.
- [10] Helmi A M, Carli R, Dotoli M, et al. Efficient and sustainable reconfiguration of distribution networks via metaheuristic optimization[J]. IEEE Transactions on Automation Science and Engineering, 2021, 19(1): 82-98.
- [11] Song Z, Li J, Jiang T, et al. Impact of photovoltaic systems on distribution networks with advances of cloud, grid and cluster computing[J]. Scalable Computing: Practice and Experience, 2023, 24(4): 1145-1156.
- [12] Ray P, Ray P K, Dash S K. Power quality enhancement and power flow analysis of a PV integrated UPQC system in a distribution network[J]. IEEE Transactions on Industry Applications, 2021, 58(1): 201-211.
- [13] Yan R, Xing Q, Xu Y. Multi-agent safe graph reinforcement learning for PV inverters-based real-time decentralized volt/var control in zoned distribution networks[J]. IEEE Transactions on Smart Grid, 2023, 15(1): 299-311.
- [14] Raouf Mohamed A A, Morrow D J, Best R J, et al. Distributed battery energy storage systems operation framework for grid power levelling in the distribution networks[J]. IET Smart Grid, 2021, 4(6): 582-598.
- [15] Huang Y, Li G, Chen C, et al. Resilient distribution networks by microgrid formation using deep reinforcement learning[J]. IEEE Transactions on Smart Grid, 2022, 13(6): 4918-4930.